

## Experimental study of woven fabrics forming defects

SHANWAN Anwar<sup>1,a \*</sup>, GHANAMEH Mohamas-Fathi<sup>1,b</sup>, BIJU Aditya<sup>1,c</sup>  
and HIVET Gilles<sup>1,d</sup>

<sup>1</sup>Laboratory of Mechanics, Orléans University, 8 rue Léonard de Vinci, 45072 Orléans, France

<sup>a</sup>anwar.shanwan@univ-orleans.fr, <sup>b</sup>mohamad-fathi.ghanameh@univ-orleans.fr,

<sup>c</sup>adityabiju99@gmail.com, <sup>d</sup>gilles.hivet@univ-orleans.fr

**Keywords:** Mesoscopic Defects, Buckles, Gapping, In-Plane Pull-Out, Woven Fabric

**Abstract.** The manufacturing of composite materials can be ensured by several industrial processes, like Liquid Composite Molding (LCM). This technology is used to produce composite parts with complex geometries because it provides a very good compromise in terms of repeatability, production rates and cost. During the forming phase of an LCM process, a fabric can be formed by highly double curved punch geometries where it could be submitted to several deformations and mechanical stresses that lead to the appearance of different types of defects: buckles, gapping, in-plane pull-out, etc. In order to understand their phenomenology, different types of defects were generated inside samples of glass and carbon fabrics so as to understand their mechanisms of appearance. This work focuses on the phenomenology of appearance of forming defects and the definition of experimental parameters allowing the generation of calibrated defects, such as buckles and gapping, inside samples of glass and carbon woven fabrics. The definition of these parameters allows the manufacturing of composite parts with calibrated defects, which in turn helps to define the influence of these defects on the mechanical behavior of composites materials.

### Introduction

Composite materials are broadly used in several industrial fields, thanks to their excellent mechanical properties. They are usually used to substitute metallic alloys due to their higher strength, lower weight and improved service life. Numerous manufacturing processes of composite materials are known in the industry [1] where the choice of a specific process depends on various criteria. The Liquid Composite Molding (LCM) process is among the most interesting processes to produce composite parts with complex geometries. In addition, this process is appropriated for the forming of fiber-reinforced polymeric composites due to its economic advantages and the capacity to produce high performance parts [2]. An LCM process has two main phases: the forming of a fabric and the injection of a liquid resin inside the formed fabric. Many research have focalized on the forming phase overall the past years [3,4] because during this phase, the fabric is subjected to several stresses that induce various deformation mechanisms such as stretching and compression, in-plane and out-of-plane bending, and shearing [5,6]. These mechanisms often lead to the appearance of several forming defects at the macroscopic scale (wrinkles) [7] and the mesoscopic scale (buckles, in-plane pull-out, and gapping) [8,9].



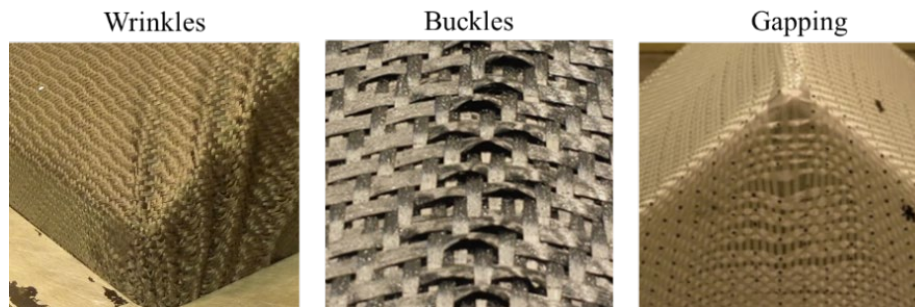


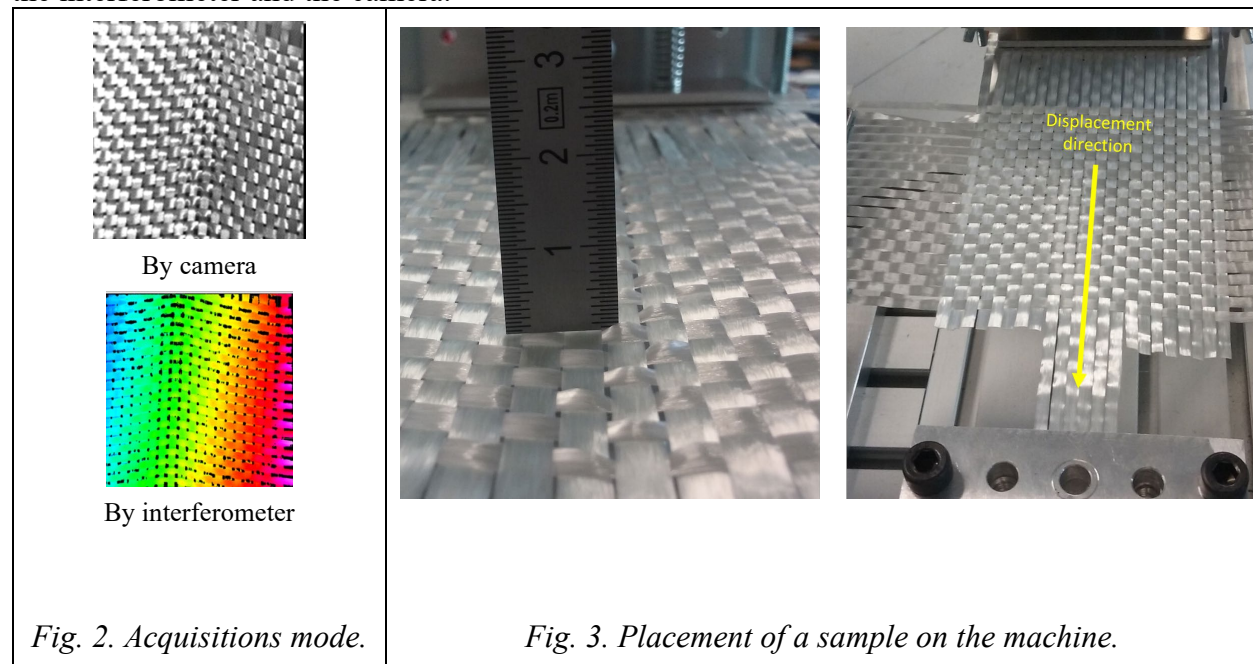
*Fig. 1. Forming defects of different types [9].*

The appearance of forming defects leads to a local heterogeneity of the preformed fabric and might impact the mechanical properties of the final composite parts. Hence, the understanding of the mechanisms of appearance of the defects seems to be crucial to avoid them or at least to reduce their magnitude. Wrinkles defects were widely studied in various studies [7,10,11]. Shanwan et al. [12] have proposed several experimental strategies to reduce their appearance or sometimes even completely avoid them. As for the mesoscopic defects, they are still not completely understood. In an interesting field of investigation, C. Tephany et al. [13] developed an experimental bench to study the buckle defects during a complex forming of a flax woven fabric. They used Digital Images Correlation (DIC) technique to accurately measure the buckle's height. Allaoui et al. [14] studied the effect of the inter-ply sliding on the buckle's appearance during the forming of woven fabrics on a prismatic tool. Capelle et al. [15] designed a specific blank holder system in order to optimize the preforming process parameters during complex geometry forming. To continue these investigations, Cruanes et al. [16] have focused on the impact of buckle defects on the mechanical properties of composite materials, specifically on the fatigue behavior. Their results showed that the orientation of buckles with respect to the tow's paths can highly reduce the mechanical performance of the composite parts. M.M. Salem et al. [17] investigated the influence of the cohesion of different woven fabrics on the reduction or prevention of the appearance of sliding defects of some vegetal and synthetic fabrics. On the other hand, Labanieh et al. [18] held an experimental and analytical research to study the mechanisms of appearance of gapping defects during the preforming of a woven carbon fabric by a hemispheric shape. Their results have demonstrated the strong effect of shear stresses and yarn tension on the appearance of gapping. Further investigations of buckles and gapping defects were carried out by Shanwan et al. [9,19] to understand and analyze these defects in depth. In order to achieve this goal, they developed a new experimental and polyvalent machine which makes it possible to produce different types of calibrated defects within samples of woven fabrics. Due to this machine, it is possible to ensure two main goals: the first one is to understand the mechanisms and criteria of appearance of forming defects while the second goal aims to produce composite parts from fabric samples containing calibrated defects, generated by the machine, of different types and amplitudes. The produced composite samples could be tested and compared with composite samples without defects. Due to this machine, the defects are generated under the same experimental parameters and the same boundary conditions that could be found during the forming phase of an LCM process. In this work, we present a new analysis of buckles, in-plane pull-out, and gapping defects, which is more developed than the one described in [9,19] where the experimental analysis was only focalized on gapping and buckles defects without referring to the in-plane pull-out. In addition, this study has experimentally approved the assumption of the previous studies [9,19] (i.e. the concomitance between the gapping and the buckles defects).

## Material and Experimental Procedure

Two types of fabrics were used for this study: the first one is a balanced plain weave glass fabric (taffetas), produced by Chomarar Company and denoted G-WEAVE 600P. This fabric has an areal weight of  $600 \text{ g/m}^2 \pm 5\%$  and a thickness of 0.55 mm. The yarn width is 3 mm and the average spacing between two yarns is 1 mm. The yarn count is 600 Tex for both the warp and the weft directions. The second fabric is a 2.5D interlock carbon fabric, denoted G1151<sup>®</sup>, produced by Hexcel company. It has a surface weight of  $630 \text{ g/m}^2$  and a unit cell of 6 warp yarns and 15 weft yarns, distributed on three levels. The tested samples are cut as a plus (+) form of  $300 \times 300 \text{ mm}^2$  with a usable central area of  $100 \times 100 \text{ mm}^2$ , as shown in Fig. 3 and Fig. 4.

The machine used in this work is equipped with four brushless AC servo motors. Each motor commands one machine axis individually, either by a force command, or by a displacement command with different speeds. Each axis is also equipped with a displacement sensor, a force sensor and two position sensors to define the beginning and the end of its stroke. In order to record the experimental parameters during the experiments, a special LabVIEW program was developed to command the machine and to ensure the acquisition of different parameters, such as the tensile forces, the speed and the position of each axis. The bench is also equipped with a digital camera and an interferometer (Gocator 3100) placed above the sample during the test. The interferometer is a three-dimensional Digital Image Correlation (DIC) system that progressively measures the height of buckles during the experiments. The acquisitions of the camera and the interferometer are adjustable to be asynchronized in order to have two information sources about the sample evolution. Fig. 2 shows an example of such acquisitions whereas Fig. 3 illustrates a sample on the bench, where the lower longitudinal and the two transverse sides of the sample are clamped by a defined and adjustable compression. However, few tows from the upper longitudinal side are completely clamped by a tight fixation and pulled at a constant speed up to a defined displacement (in-plane pull-out in the direction of the yellow arrow in Fig. 3). This displacement simulates the same movement of the tows in contact with the punch during the forming phase of an LCM process. During the experiments, the forces and the displacements of each axis are continuously recorded by a LabVIEW program and synchronized with a simultaneous acquisition of images of the interferometer and the camera.



## Results and Discussion

The results of this section confirm a previous expectation that we assumed during the studies [9] and [19] about the concomitance between buckles and gapping defects. In addition, this study presents a detailed investigation to better understand the interactions between the displacement of the longitudinal yarns and the deformation of the transverse yarns and its influence on the possible appearance of buckles and gapping defects. These investigations are explained by means of Fig. 4 and Fig. 5. As shown by Fig. 5, the displacement of the pulled longitudinal yarns leads to a displacement of the transverse yarns due to the friction between the two networks of the fabric yarns. Subsequently, an in-plane bending of the transverse yarns takes place in the useful area of the sample, whereas the parts of the same yarns, which are clamped between the transverse jaws, do not rotate because of the static friction between the metal and the yarns. When the traction force, transmitted to the transverse yarns, overcomes the static friction between the metallic jaws and the fabric, the transverse yarns between the jaws rotate and continue their in-plane bending.

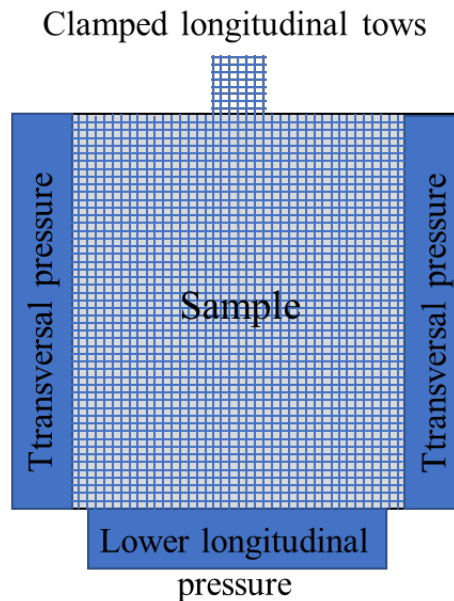


Fig. 4. Form of the prepared samples before the experiments.

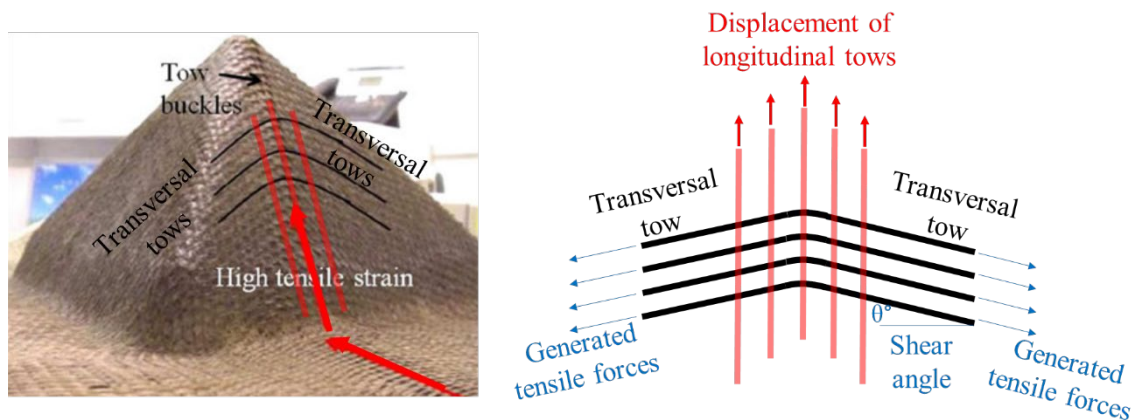


Fig. 5. Phenomenology of appearance of the forming defects [9].



Depending on the bending stiffness of the yarns, the in-plane bending continues until a defined shear angle where it stops and becomes an out-of-plane bending of the transverse yarns. It is at this moment that the buckle defects appear. Then, the amplitude of buckles increases until the end of the first phase which ends at the peak of the curve force/displacement, as shown in Fig. 6. At this moment, the traction force applied on the yarns overcomes the static friction between the fabrics yarns (cohesion) where a relative sliding of the longitudinal yarns takes place with respect to the transverse ones. This moment announces the beginning of the second phase (in-plane pull-out). Depending on the homogeneity of the transverse pressure, applied on the transverse yarns, and/or the regularity of the sample thickness, the displacement of the longitudinal yarns provokes either a simple pull-out of these yarns from the fabric or a displacement of some transverse yarns with the pulled longitudinal ones with respect to the other transverse yarns. In this last case, we observe the formation of some gaps inside the sample which lead to the appearance of weave pattern heterogeneity defects, sometimes called decohesion or even gapping defects. The second phase is also characterized by many oscillations due to a stick-slip phenomenon. Finally, the third phase of the curve starts at the beginning of the loss of contact between the lower part of the sample and the metallic jaws that clamp it. This phase continues until the sample is no longer held between the jaws.

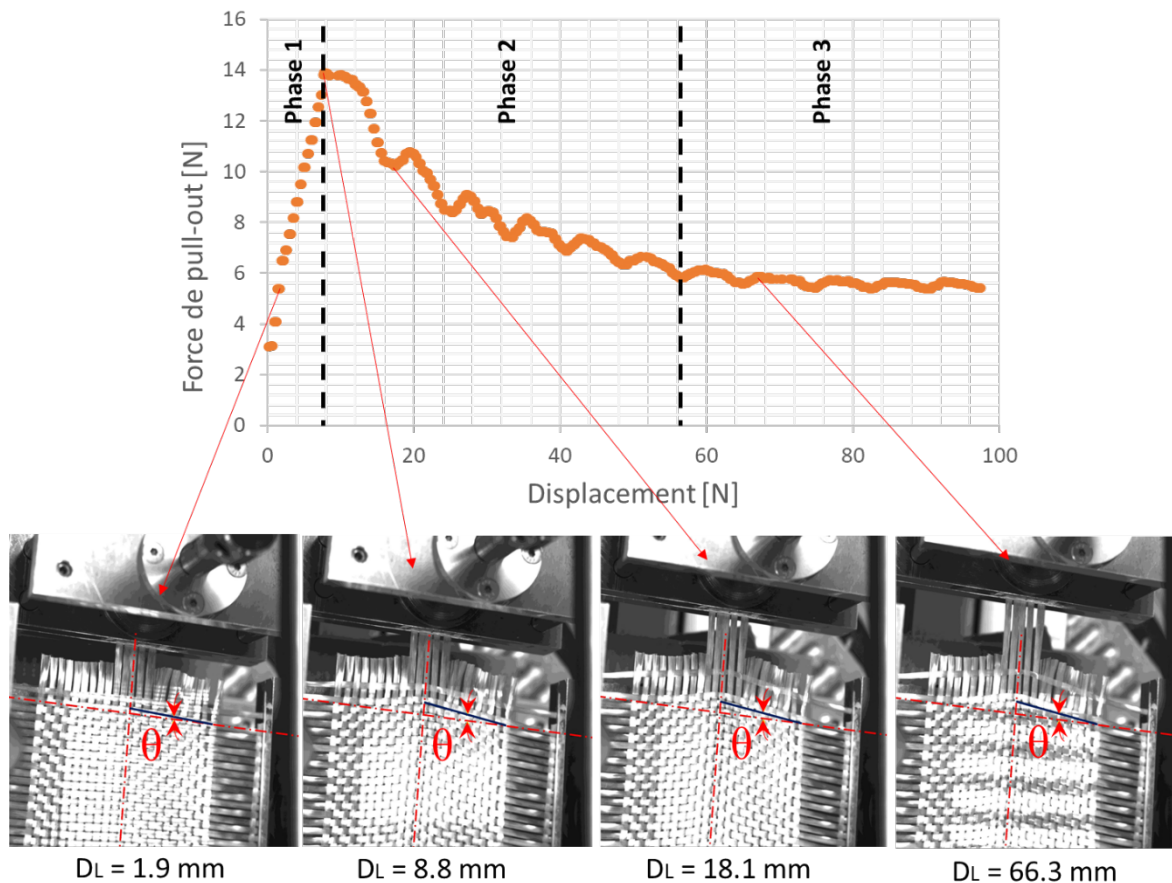


Fig. 6. Different phases of preforming defects appearance.

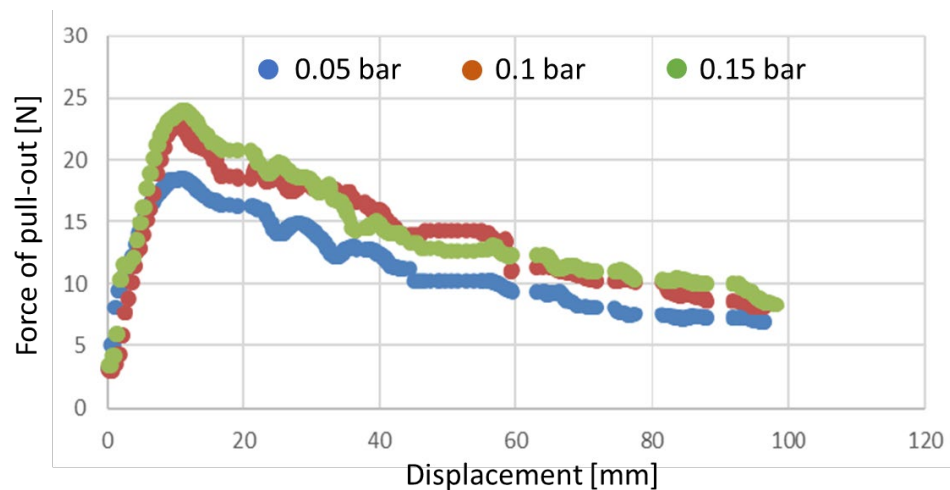
The above-mentioned phenomenology was verified by a measurement of displacements of the transverse yarns, directly executed on the recorded images (Fig. 6), by means of the ImageJ software. The measurements showed that the shear angle  $\theta^\circ$  increases during the phase 1, up to  $13^\circ$ , then it remains constant during the other two phases. The measured values are presented in

Table 1, where  $D_L$  and  $D_T$  respectively refer to the displacement of the longitudinal and the transverse yarns.

*Table 1. Relationship between the yarn's displacements and the shear angle.*

Phase 1			Phase 2	Phase 3
$D_L = 0$	$D_L = 1.9 \text{ mm}$	$D_L = 8.8 \text{ mm}$	$D_L = 18.8 \text{ mm}$	$D_L = 66.3 \text{ mm}$
$D_T = 0$	$D_T = 2.1 \text{ mm}$	$D_T = 5.2 \text{ mm}$	$D_T = 5.2 \text{ mm}$	$D_T = 5.2 \text{ mm}$
$\theta^\circ = 0^\circ$	$\theta^\circ = 8.6^\circ$	$\theta^\circ = 13^\circ$	$\theta^\circ = 13^\circ$	$\theta_s = 13^\circ$

Next, the appearance of defects was investigated on two types of fabrics, as a function of four experimental parameters: the number of the pulled tows, the transverse compression, the longitudinal compression, and the speed of displacement of the pulled longitudinal yarns. Each parameter was tested at three different values with a repeatability of three experiments per value while the other parameters were fixed for each tested parameter. In total, 36 experiences were carried-out for each type of fabric (4 parameters \* 3 values \* 3 repeatability). Fig. 7 shows an example of one set of such experiments, carried-out on a cross glass fabric sample, where the transverse pressure was set at 0.05, 0.10, and 0.15 bars whereas the other experimental parameters were fixed as follows: The lower longitudinal pressure = 0.05 bar, The speed of displacement = 1 mm/sec, and the number of pulled tows = 7. The choice of these parameters was selected as those of a forming process.



*Fig. 7. Evolution of the pull-out force of the upper longitudinal yarns with the displacement.*

As shown by these curves, an increase of the transverse pressure leads to an increase in the pull-out force of the longitudinal yarns. This increase is very logical as the traction force should overcome the friction between the fabric and the blank holder which increases with the normal pressure according to the Coulomb's law of friction. The tests presented by these curves corresponded to the appearance of buckles and gapping defects, with respect to the above-mentioned parameters. Fig. 8 shows an example of buckles and gapping appearance.

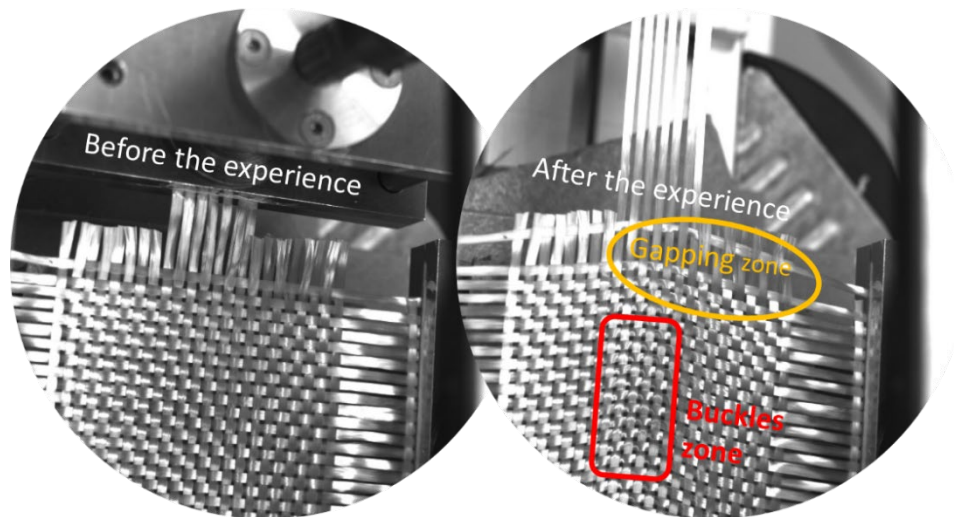


Fig. 8. Appearance of buckles and gapping defects on samples of glass fabric.

The Table 2 presents the group of experiments that studies the influence of the transverse pressure evolution on the defect's appearance. The experiments were repeated for three numbers of the pulled tows (3, 5, and 7) whereas the other experimental parameters were kept constant as follows: the longitudinal pressure = 0.05 bar, and the speed of displacement = 1 mm/sec. Thus, the Table 2 contain 9 series of experiences. In this table the symbol (✓) refers to the appearance of the defects whereas the symbol (x) indicates to a non-appearance of defects. Many deep analyses could be done but at this stage of the study we focalized on the definition of the experimental parameters allowing the appearance of forming defects and the comparison between the influence of these parameters on the defect's appearance for two types of fabrics.

Table 2. Experiments parameters allowing the appearance of buckles and gapping in glass fabric samples.

Number of tows	Transverse Pressure ( $P_T$ )	Buckles	Gapping
3	0.05 bar	x	x
	0.1 bar	□	x
	0.15 bar	□	x
5	0.05 bar	□	x
	0.1 bar	□	x
	0.15 bar	□	x
7	0.05 bar	□	□
	0.1 bar	□	□
	0.15 bar	□	□

For the other experimental parameters, the influence of their evolution on the forming process was also tested. The Fig. 9 shows, for example, whether the velocity of pull-out has an influence on the pull-out force. The curves show a decrease in the pull-out force if the velocity increases and

the ratio of the force reduction is almost proportional to the ratio of increase in the velocity. This result needs a deeper analysis with other effects that should be considered, like the dynamic effect, the variability related to the heterogeneous behavior the fibrous structures.

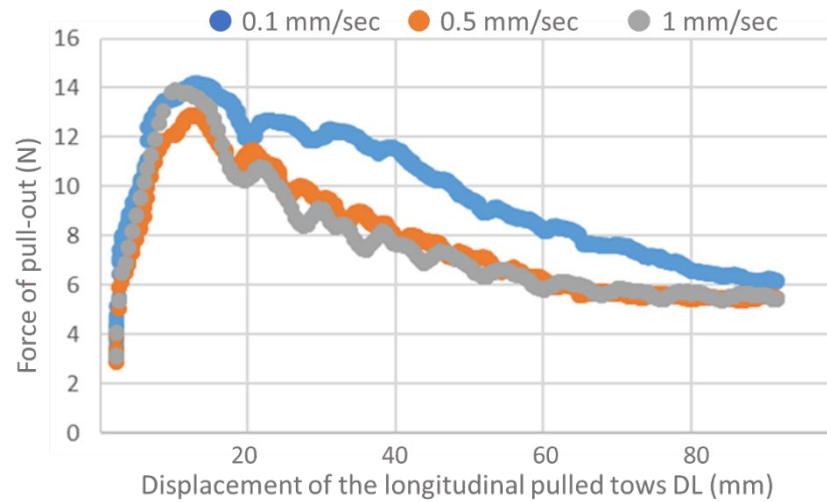


Fig. 9. Influence of the pull-out velocity on the pull-out force evolution.

Finally, when applying the same experimental parameters, that allowed the appearance of buckles and gapping defects in the case of glass fabric samples, on samples of the interlock carbon fabric G1151, it was possible to generate buckles defects only, without any appearance of gapping. Consequently, it can be concluded that the appearance of preforming defects is not only related to the experimental parameters, but also to the cohesion of the fabric as well as the boundary conditions during the process. This conclusion was indeed confirmed by the experiences presented in Fig. 10 that shows two examples of forming experiments on carbon and glass fabrics where both tests were executed under the same following conditions which are as follows: width of the pulled tows =  $25 \pm 2$  mm, displacement speed = 1 mm/sec, transverse pressure = 0.15 bar, and the longitudinal pressure = 0.05 bar.

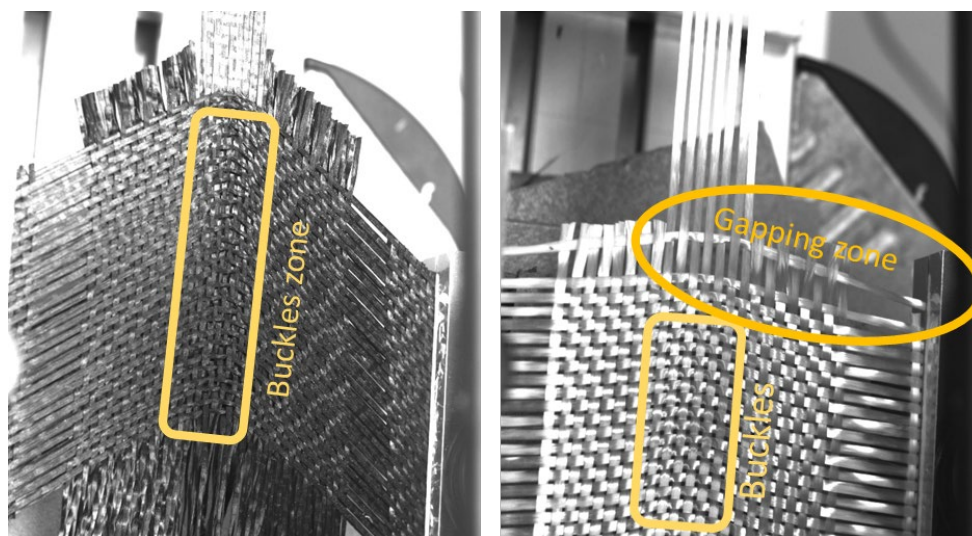


Fig. 10. Generated defects on glass and carbon fabrics.



## Summary

This research contributed to the understanding of preforming defects and their mechanisms of appearance. It has been demonstrated that buckles, gapping and/or pull-out defects could not be separated even if it is sometimes possible to generate this or that defect. These defects are always concomitant and the appearance of one or both of them depends on the experimental parameters, the boundary conditions and the cohesion of the tested fabric.

## References

- [1] Y. Li, Y. Xiao, L. Yu, K. Ji, D. Li, A review on the tooling technologies for composites manufacturing of aerospace structures: materials, structures and processes, *Compos. Part A: Appl. Sci. Manuf.* 154 (2022) 106762. <https://doi.org/10.1016/j.compositesa.2021.106762>
- [2] S. Konstantopoulos, C. Hueber, I. Antoniadis, J. Summerscales, R. Schledjewski, Liquid composite molding reproducibility in real-world production of fiber reinforced polymeric composites: a review of challenges and solutions, *Adv. Manuf. Polym. Compos. Sci.* 5 (2019) 85-99. <https://doi.org/10.1080/20550340.2019.1635778>
- [3] P. Boisse, R. Akkerman, P. Carlone, L. Kärger, S.V. Lomov, J.A. Sherwood, Advances in composite forming through 25 years of ESAFORM, *Int. J. Mater. Form.* 15 (2022) 39. <https://doi.org/10.1007/s12289-022-01682-8>
- [4] B. Liang, P. Boisse, A review of numerical analyses and experimental characterization methods for forming of textile reinforcements, *Chin. J. Aeronaut.* 34 (2021) 143-163. <https://doi.org/10.1016/j.cja.2020.09.027>
- [5] R. Bai, B. Chen, J. Colmars, P. Boisse, Physics-based evaluation of the drapability of textile composite reinforcements, *Compos. Part B Eng.* 242 (2022) 110089. <https://doi.org/10.1016/j.compositesb.2022.110089>
- [6] F. Nosrat Nezami, T. Gereke, C. Cherif, Analyses of interaction mechanisms during forming of multilayer carbon woven fabrics for composite applications, *Compos. Part Appl. Sci. Manuf.* 84 (2016) 406-416. <https://doi.org/10.1016/j.compositesa.2016.02.023>
- [7] P. Boisse, J. Huang, E. G-Maldonado, Analysis and Modeling of Wrinkling in Composite Forming, *J. Compos. Sci.* 5 (2021) 3. <https://doi.org/10.3390/jcs5030081>
- [8] R. Azzouz, S. Allaoui, R. Moulart, Composite preforming defects: a review and a classification, *Int. J. Mater. Form.* 14 (2021) 1259-1278. <https://doi.org/10.1007/s12289-021-01643-7>
- [9] A. Shanwan, S. Allaoui, J. Gillibert, G. Hivet, Development of an experimental approach to study preforming mesoscopic defects of woven fabrics, 24th International Conference on Material Forming, Liège, Belgium, Apr. 2021. <https://doi.org/10.25518/esaform21.1580>
- [10] S. Chen, O. P.L. McGregor, L.T. Harper, A. Endruweit, N.A. Warrior, Defect formation during preforming of a bi-axial non-crimp fabric with a pillar stitch pattern, *Compos. Part A : Appl. Sci. Manuf.* 91 (2016) 156-167. <https://doi.org/10.1016/j.compositesa.2016.09.016>
- [11] P. Boisse, N. Hamila, A. Madeo, Modelling the development of defects during composite reinforcements and prepreg forming, *Philos. Transact. A Math. Phys. Eng. Sci.* 374 (2016) 20150269. <https://doi.org/10.1098/rsta.2015.0269>
- [12] A. Shanwan, S. Allaoui, Different experimental ways to minimize the preforming defects of multi-layered interlock dry fabric, *Int. J. Mater. Form.* 12 (2019) 69-78. <https://doi.org/10.1007/s12289-018-1407-6>
- [13] C. Tephany, J. Gillibert, P. Ouagne, G. Hivet, S. Allaoui, D. Soulat, Development of an experimental bench to reproduce the tow buckling defect appearing during the complex shape forming of structural flax based woven composite reinforcements, *Compos. Part Appl. Sci. Manuf.* 81 (2016) 22-33. <https://doi.org/10.1016/j.compositesa.2015.10.011>
- [14] S. Allaoui, C. Cellard, G. Hivet, Effect of inter-ply sliding on the quality of multilayer interlock dry fabric preforms, *Compos. Part Appl. Sci. Manuf.* 68 (2015) 336-345. <https://doi.org/10.1016/j.compositesa.2014.10.017>

- [15] E. Capelle, P. Ouagne, D. Soulat, D. Duriatti, Complex shape forming of flax woven fabrics: Design of specific blank-holder shapes to prevent defects, *Compos. Part B Eng.* 62 (2014) 29-36. <https://doi.org/10.1016/j.compositesb.2014.02.007>
- [16] C. Cruanes, A. Shanwan, S. Méo, S. Allaoui, M-P. Deffarges, F. Lacroix, G. Hivet, Effect of mesoscopic out-of-plane defect on the fatigue behavior of a GFRP, *Mech. Mater.* 117 (2018) 214-224. <https://doi.org/10.1016/j.mechmat.2017.11.008>
- [17] M.M. Salem, E. De Luycker, K. Delbe, M. Fazzini, P. Ouagne, Experimental investigation of vegetal and synthetic fabrics cohesion in order to prevent the tow sliding defect via frictional and pull-out test, *Compos. Part Appl. Sci. Manuf.* 139 (2020) 106083. <https://doi.org/10.1016/j.compositesa.2020.106083>
- [18] A.R. Labanieh, C. Garnier, P. Ouagne, O. Dalverny, D. Soulat, Intra-ply yarn sliding defect in hemisphere preforming of a woven preform, *Compos. Part Appl. Sci. Manuf.* 107 (2018) 432-446. <https://doi.org/10.1016/j.compositesa.2018.01.018>
- [19] A. Shanwan, S. Allaoui, J. Gillibert, G. Hivet, Development and Implementation of an Experimental Machine to Study Woven Fabric Preforming Defects, *Exp. Tech.* 46 (2022) 299-316. <https://doi.org/10.1007/s40799-021-00483-z>